doi:10.1246/cl.2010.1004

Reversible Aggregation and Deaggregation of Helicene-grafted Chiral Silica Nanoparticles Induced by Aromatic Solvents

Zengjian An,[1] Yoshizumi Yasui,[1] Takanari Togashi,[1] Tadafumi Adschiri,[1,2] Shunpei Hitosugi,[3]
Hiroyuki Isobe,[3] Takeshi Higuchi,[1] Masatsugu Shimomura,[1,2] and Masahiko Yamaguchi*[1,4]
[1]*WPI-Advanced Institute for Materials Research, Tohoku University,*
2-1-1 Katahira, Aoba-ku, Sendai, Miyagi 980-8577
[2]*Institute of Multidisciplinary Research for Advanced Materials, Tohoku University,*
2-1-1 Katahira, Aoba-ku, Sendai, Miyagi 980-8577
[3]*Department of Chemistry, Graduate School of Science, Tohoku University, Aoba-ku, Sendai, Miyagi 980-8578*
[4]*Department of Organic Chemistry, Graduate School of Pharmaceutical Sciences, Tohoku University,*
Aoba-ku, Sendai, Miyagi 980-8578

(Received June 8, 2010; CL-100538; E-mail: yama@mail.pharm.tohoku.ac.jp)

Silica nanoparticles with sizes of 210 and 440 nm were grafted with (*P*)- or (*M*)-1,12-dimethylbenzo[*c*]phenanthrenes by silane coupling with helicenamidated (3-aminopropyl)trimethoxysilane. The chiral nanoparticles deaggregated and aggregated with sonication in soft and hard aromatic solvents.

Nanoparticles have attracted much interest because of their potential application in biology, chemistry, and material sciences. However, they exhibit uncontrolled aggregation,[1] which hampers their practical use. Grafting nanoparticles with functional molecules have been employed to control aggregation.[2–6] In this process, notable is the reversible aggregation and deaggregation resulting from nonconvalent bonding interactions of the grafted molecules, which include hydrogen bonds, electrostatic interactions, and hydrophilic–hydrophobic-phase transition. In general, the specific affinity of biomolecules such as DNA,[2] peptides,[3] proteins,[4] and sugars[5] is employed. The use of synthetic organic molecules to control aggregation between nanoparticles, however, is less common, but the development of such a method would broaden the scope of the reversible assembly of nanoparticles on nanometer and micrometer scales. In this work, novel helicene-grafted-chiral-silica nanoparticles were synthesized, the aggregation and deaggregation of which were related to our previous findings that ethynylhelicene oligomers form double-helices in hard aromatic solvents and unfold in soft solvents.[7]

Silica nanoparticles with sizes of 210 and 440 nm[8] were reacted with *N*-[3-(trimethoxysilyl)propyl]-8-methoxycarbonyl-1,12-dimethylbenzo[*c*]phenanthrene-5-carboxyamide (**1**) at 100 °C in ethanol. (*P*)-Nanoparticles and (*M*)-nanoparticles were obtained from (*P*)-**1** and (*M*)-**1** (ee >99%). These called (*P*)-balls and (*M*)-balls, respectively, in this work (Figure 1). Characterizations of IR, UV–vis, CD, and TG proved the presence of (*M*)- and (*P*)-helicenes on nanoparticles (Figures 1S–4S).[9] The graft loading was 0.2 mmol g^{-1} for 440-nm nanoparticles by TG, and it was 0.4 mmol g^{-1} for 210 nm (Figures 1S–4S, see Supporting Information).[9]

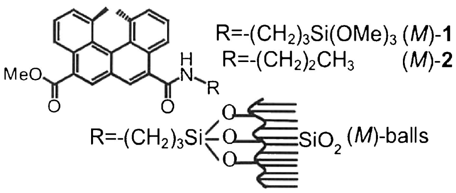

Figure 1. Structure of (*M*)-helicene derivatives and (*M*)-balls.

The 440-nm (*M*)-balls could be dispersed in *N*,*N*-dimethylformamide (DMF) by sonication, as indicated by transmission electron microscopy (TEM) (Figure 5Sa).[9] The solubility of the nanoparticles in DMF was high, and solution was homogeneous even at 5 mg mL^{-1}. No aggregation occurred in 0.2-mg mL^{-1} solution for over one week. However, when it was acidified to pH 1 by adding 1 M hydrochloric acid, aggregation quickly occurred to form precipitate, which was detected by TEM and dynamic light scattering (DLS) (Figure 5Sb and Figure 6S).[9] DMF solution of ungrafted-silica nanoparticles was stable under neutral and acidic conditions (pH 1), which indicated that silanol groups on the nanoparticle surface had a small effect on the acid-driven aggregation. The grafted helicene should have played important roles in this aggregation. When the precipitate was collected and dissolved in DMF by sonication, they deaggregated to dispersion (Figure 5Sc).[9]

The effect of aromatic solvents was noted in reversible aggregation using iodobenzene, bromobenzene, chlorobenzene, toluene, and benzotrifluoride (α,α,α-trifluorotoluene). The precipitate of the 440-nm (*M*)-balls formed at pH 1 was separated by centrifugation, and sonicated in aromatic solvents (0.2 mg mL^{-1}) for 10–30 min. The precipitate disappeared in iodobenzene, and a dispersed solution was obtained, which was confirmed by DLS (Figure 2). The average sizes showed no obvious change after 3 days. In bromobenzene, a mixture was formed containing 40% blocks of 5000 nm and 60% dispersed nanoparticles. Aggregate size increased to 1000 nm in chlorobenzene and to 3800 nm in toluene. Aggregates with a number-average size of 5400 nm were formed in benzotrifluoride. Sonication was essential for this process, and no change occurred for the pH 1 precipitate without sonication. The TEM images were consistent with the DLS results of the aggregated

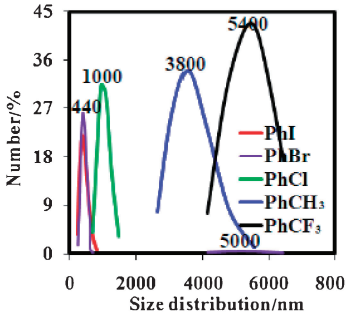

Figure 2. DLS (0.2 mg mL^{-1}, scattering angel: 173°, 20 °C) of 440-nm (*M*)-balls in aromatic solvents.

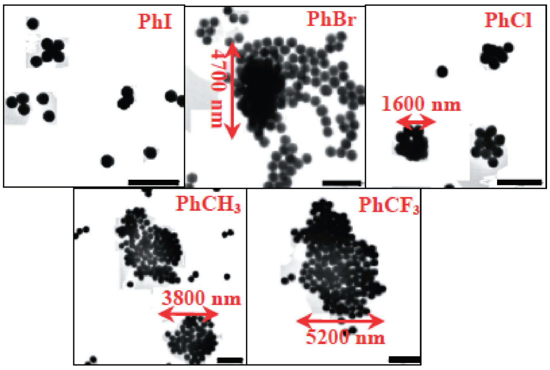

Figure 3. TEM images (bar scale: 2 µm) of 440-nm (*M*)-balls in aromatic solvents.

Table 1. Effect of concentration on the aggregation of 440-nm (*M*)-balls analyzed by DLS (scattering angel: 173°, 20 °C)

Solvent	Size distribution/nm Concentration/mg mL^{-1} 0.1	 0.2		 0.4	 1.0
PhI	400	440	640^a	650	2000
PhBr	400/4500 (30%/70%)	440/5000 (60%/40%)	820^a	1300	5500
PhCl	1400	1000	1100^a	2500	Precip^b
PhCH$_3$	3700	3800	2500^a	5400	Precip^b
PhCF$_3$	5200	5400	—	Precip^b	Precip^b

^{a}Sizes of aggregates formed from 5400-nm blocks in benzotrifluoride. ^{b}Precip: precipitate formation.

structures (Figure 3). The enantiomeric (*P*)-balls showed similar results to the (*M*)-balls (Figure 7S).[9]

The degree of aggregation depended on concentration. In iodobenzene, the average size of the aggregate blocks detected by DLS was 650 nm at 0.4 mg mL^{-1} (Table 1 and Figure 9S).[9] At 1.0 mg mL^{-1}, aggregate size increased to 2000 nm (Figure 10S).[9] An increase in aggregate size was also observed in bromobenzene, chlorobenzene, toluene, and benzotrifluoride. In benzotrifluoride, marked precipitation occurred at 0.4 mg mL^{-1}. The degree of aggregate could be controlled using soft and hard aromatic solvents as well as using appropriate concentrations. Similar aggregation and deaggregation were observed by DLS for the 210 nm (*P*)-balls at 0.2 mg mL^{-1} (Table 1S and Figures 11S–13S).[9]

Aggregate size could be changed not only for the pH 1 precipitate but also for the 5400-nm blocks in benzotrifluoride: the 5400-nm blocks of 440-nm (*M*)-balls formed in benzotrifluoride were separated by centrifugation, and sonicated in different aromatic solvents (0.2 mg mL^{-1}) for 10–30 min. DLS showed that aggregate size decreased in toluene, chlorobenzene, bromobenzene, and iodobenzene in this order (Figure 4).

The CD spectra of 440-nm (*M*)-balls in bromobenzene, chlorobenzene, and benzotrifluoride revealed an increase in the Cotton effect at 317 nm with increasing degree of aggregation (Figure 5). The aggregation, which could be detected by CD, may be caused by the π–π interactions of helicenes grafted to the nanoparticle surface.

In summary, helicene-grafted-chiral-silica nanoparticles were synthesized, and their reversible aggregation and deaggregation were conducted in hard and soft aromatic solvents. To the best of our knowledge, no such strong solvent dependence on nanoparticle aggregation in organic solvents has been reported yet. Studies of related nanoparticles will be an interesting work for future research.

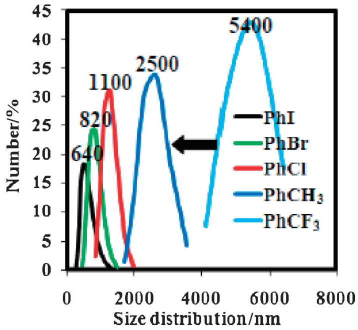

Figure 4. Deaggregation experiments of 440-nm (*M*)-balls in benzotrifluoride to iodobenzene, bromobenzene, chlorobenzene, and toluene analyzed by DLS (0.2 mg mL^{-1}, scattering angel: 173°, 20 °C).

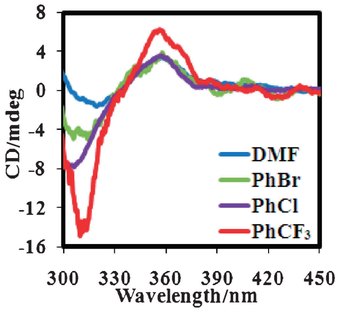

Figure 5. CD spectra (1.0 mg mL^{-1}, 25 °C) of 440-nm (*M*)-balls in solvents.

Financial support from WPI-AIMR Fusion Research, JSPS (No. 22790004) and G-COE are acknowledged, and authors also thank Mr. Masaki Ageishi, Ms. Mika Kanehira, and Mr. Yoshiro Shibata (Institute of Multidisciplinary Research for Advanced Materials, Tohoku University) for TEM.

References and Notes

1 R. P. Bagwe, L. R. Hilliard, W. Tan, *Langmuir* **2006**, *22*, 4357.
2 C. A. Mirkin, R. L. Letsinger, R. C. Mucic, J. J. Storhoff, *Nature* **1996**, *382*, 607.
3 D. Aili, K. Enander, J. Rydberg, I. Lundström, L. Baltzer, B. Liedberg, *J. Am. Chem. Soc.* **2006**, *128*, 2194; N. Nath, A. Chilkoti, *J. Am. Chem. Soc.* **2001**, *123*, 8197.
4 S. Cobbe, S. Connolly, D. Ryan, L. Nagle, R. Eritja, D. Fitzmaurice, *J. Phys. Chem. B* **2003**, *107*, 470.
5 J. M. de la Fuente, A. G. Barrientos, T. C. Rojas, J. Rojo, J. Cañada, A. Fernández, S. Penadés, *Angew. Chem., Int. Ed.* **2001**, *40*, 2257; H. Otsuka, Y. Akiyama, Y. Nagasaki, K. Kataoka, *J. Am. Chem. Soc.* **2001**, *123*, 8226.
6 T. Kim, K. Lee, M. Gong, S. Joo, *Langmuir* **2005**, *21*, 9524.
7 H. Sugiura, Y. Nigorikawa, Y. Saiki, K. Nakamura, M. Yamaguchi, *J. Am. Chem. Soc.* **2004**, *126*, 14858.
8 R. D. Badley, W. T. Ford, F. J. McEnroe, R. A. Assinks, *Langmuir* **1990**, *6*, 792.
9 Supporting Information is available electronically on the CSJ-Journal Web site, http://www.csj.jp/journals/chem-lett/index.html; synthesis and grafting procedures; characterizations by IR, UV–vis, CD, TG, and DLS; and results of DLS, TEM, and CD.